PROCEEDINGS OF SCIENCE

Probing the intrinsic heavy quark content of the nucleon through direct photon plus heavy quark production

Tzvetalina STAVREVA*
Laboratoire de Physique Subatomique et de Cosmologie, UJF, CNRS/IN2P3, INPG, 53 avenue des Martyrs, 38026 Grenoble, France
E-mail: stavreva@lpsc.in2p3.fr

The associated production of a direct photon with a heavy quark provides us with the opportunity to test for and constrain the presence of intrinsic charm and bottom in the nucleon. We present comparisons of the theoretical predictions for this process with measurements at the Tevatron. Future predictions and possibilities for measurement of the process at the LHC and the potential for constraining the heavy quark patron distributions there are presented.

XXI International Workshop on Deep-Inelastic Scattering and Related Subjects
22-26 April, 2013
Marseilles, France

*Speaker.

PoS(DIS 2013)303

1. Introduction

1.1 Direct $\gamma + Q$

In order to gather more information on the heavy quark PDFs it is important to investigate in detail processes sensitive to them. Direct photon production in association with a heavy quark (c or b) is exactly one such process due to its dependence on subprocesses sensitive to the initial state heavy quark (HQ) distributions [1].

At LO it has a simple form – it consists of one hard-scattering subprocess, $g + Q \to \gamma + Q$ (Compton subprocess), and also fragmentation contributions[1], these being greatly suppressed due to experimental isolation requirements. At NLO the number of contributing hard-scattering subprocesses increases to seven [2]:

$$\begin{array}{ll} g+g \to Q+\bar{Q}+\gamma & Q+Q \to Q+Q+\gamma \\ g+Q \to g+Q+\gamma & Q+\bar{Q} \to Q+\bar{Q}+\gamma \\ Q+q \to q+Q+\gamma & q+\bar{q} \to Q+\bar{Q}+\gamma \\ Q+\bar{q} \to Q+\bar{q}+\gamma & \end{array}$$

also including NLO fragmentation effects, which are small due to the isolation cuts as in the LO case. Given that most of the subprocesses are initiated by either heavy quarks or gluons, and in the proton the gluon distribution is well known, it is possible to focus on constraining the heavy quark PDF through measurements of this process.

1.2 Intrinsic Charm

In the standard global analysis of PDFs, heavy quarks do not have free fit parameters associated with them. It is assumed that the heavy quark PDF can be obtained purely perturbatively through the use of the DGLAP evolution equations, having set an appropriate initial condition. However there is no theoretical reason that this should be the case and moreover there have been some data that point towards the existence of an intrinsic charm component in the proton (F_2^c at large x as measured by EMC [2]). As a result there are non-perturbative models predicting the size and shape of the intrinsic heavy quark component [3, 4] which are used in PDF global fits[3] [5]. In Fig. 1 the difference between different IC PDFs and the radiatively radiate charm (CTEQ6.6M) is displayed. Both the BHPS (dashed red line) and Meson Cloud model (dotted green line) show a similar behavior where they peak at high x. The purely phenomenologically inspired sea-like model (dash-dotted blue line) produces a PDF which is larger than the radiatively generated one in a broad x range. In order to constrain precisely the HQ PDF it is important to measure processes sensitive to it such as $\gamma + Q$. How these different models affect the $\gamma + Q$ cross-section is presented in the next section.

[1] The LO fragmentation contributions consist of all $2 \to 2$ subprocesses of order $\mathcal{O}(\alpha_s^2)$ containing at least one heavy quark in the final state convoluted with the photon fragmentation function $D_{\gamma/q,g}(z, Q^2)$.

[2] This calculation is performed in the variable flavor number scheme, where the heavy quarks are treated as massless.

[3] Currently there are fits available only for IC. The IB/IC ratio is expected to be proportional to m_c^2/m_b^2.

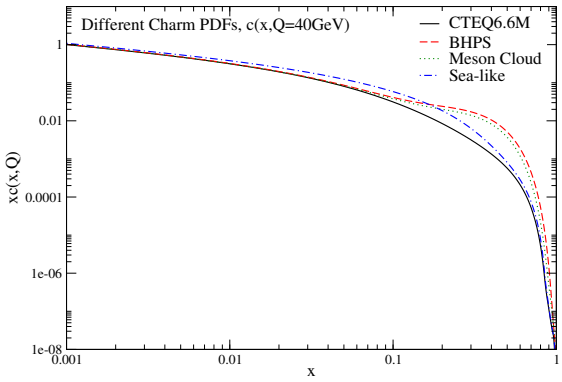

Figure 1: Comparison between the radiatively generated charm PDF (CTEQ6.6M, solid black line), charm PDF including IC: under the BHPS model (CTEQ6.6C1, dashed red line), under the Meson Cloud model (CTEQ6.5C4, dotted green line), under the sea-like model (CTEQ6.6C3, dash-dotted blue line)

2. Predictions: hadron-hadron collisions

2.1 Tevatron

The differential cross-section vs $p_{T\gamma}$ for $\gamma+c$ and $\gamma+b$ production at the Tevatron is presented at both NLO and LO in Fig. 2. From there we see that the difference between $d\sigma^{\gamma+c}/dp_{T\gamma}$ and $d\sigma^{\gamma+b}/dp_{T\gamma}$ at LO stays almost constant, whereas it decreases at NLO with growing $p_{T\gamma}$. The reason for this is that at the Tevatron, due to the abundance of valence quarks and anti-quarks, the annihilation subprocess ($q+\bar{q}\rightarrow Q+\bar{Q}+\gamma$) starts to dominate the cross-section, and this subprocess is exactly the same for both $\gamma+c$ and $\gamma+b$ production. When one looks at the comparison between theory and experimental measurements (performed by the DØ collaboration [6]) in Fig. 3, the agreement for $\gamma+b$ is very good, whereas for $\gamma+c$ the data overshoot the theoretical predictions at high p_T. One possibility to try and correct for this discrepancy is to utilize IC PDFs in the theoretical predictions. In Fig. 4 the data over theory ratio is presented, as well as the ratios $\frac{d\sigma^{BHPS}/dp_{T\gamma}}{d\sigma^{CTEQ6.6M}/dp_{T\gamma}}$, $\frac{d\sigma^{sea-like}/dp_{T\gamma}}{d\sigma^{CTEQ6.6M}/dp_{T\gamma}}$. As expected the sea-like cross-section overshoots the data at low p_T, but undershoots it at high p_T. Conversely the BHPS cross-section, follows the data trend, and provides a better description than both the radiatively generated charm and the sea-like charm cross-section, however it still undershoots the data at very high p_T. For the $\gamma+b(jet)$ production in [6] and [7] there was no enhancement observed in the p_T^{γ}-spectrum, however in later measurements [8] the DØ collaboration observed such an enhancement.

2.2 LHC

Due to the higher center of mass energy at the LHC with respect to the Tevatron, reaching high - x ($x\sim p_T/\sqrt{S}$) requires probing forward particle rapidities. Therefore in order to explore the ranges which are sensitive to IC, we present predictions for both central and forward photon rapidities. Utilizing experimental cuts appropriate for the ATLAS detector shown in Table 1 we

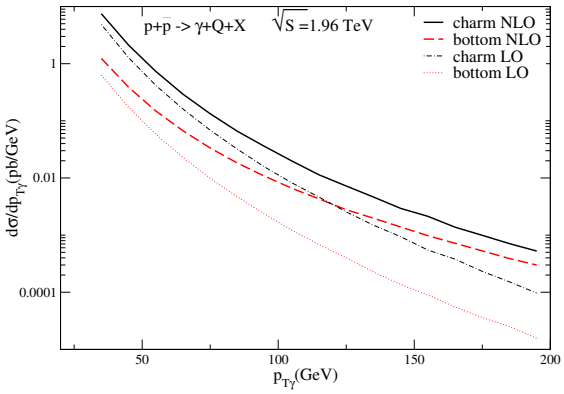

Figure 2: $d\sigma^{\gamma+Q}/dp_{T\gamma}$: for charm at NLO (black solid line), at LO (black dash-dotted line), for bottom at NLO (red dashed line), at LO (red dotted line).

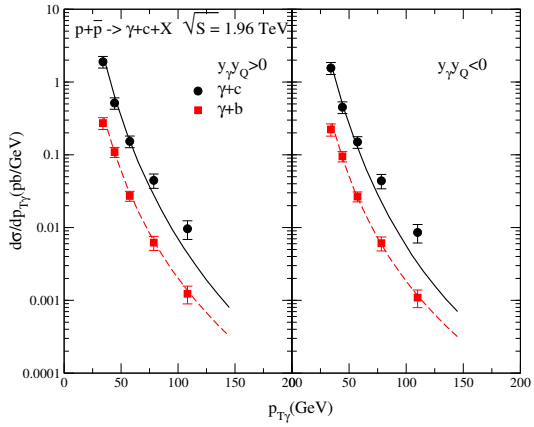

Figure 3: Comparison between theory - $\gamma+c$ (solid black curve), $\gamma+b$ (dashed red curve) and DØ data - $\gamma+c$ (black circles), $\gamma+b$ (red squares).

present in Fig. 5 and Fig. 6 the predictions respectively for the central and forward photon rapidity region [9]. There the solid blue line represents the differential cross-section calculated with the radiatively generated charm PDF (cteq6.6M), the dash-dotted green line uses as input the sea-like PDF (cteq66c4) and the dashed red line the BHPS PDF (cteq66c2). In the lower half of Fig. 5 the above distributions normalized to the distribution acquired using the cteq6.6M PDF and $\mu_r = \mu_f = \mu_F = p_T^\gamma$, are presented. The shaded yellow region, represents the scale dependence. It is clearly visible that as p_T^γ grows so does the difference between the distributions using the IC PDFs and the one using CTEQ66. Clearly the difference between the spectrum using the BHPS IC PDF and the one using the radiatively generated PDF increases as p_T^γ increases, however in this central rapidity region at $p_T^\gamma \sim 400$ GeV the BHPS IC and sea-like IC spectra are roughly the same.

In Fig. 6 the same distributions as in Fig. 5 are shown, however for forward photon rapidity

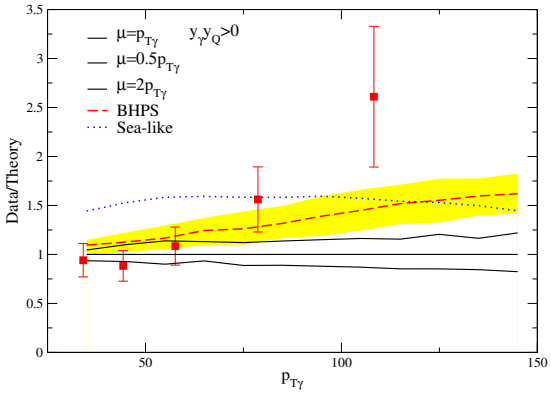

Figure 4: Data over theory ratio for $\gamma + c$ production (red squares), the theoretical predictions are for radiatively generated charm including the scale dependence (black lines), BHPS IC (red dashed line), sea-like IC (blue dotted line).

	p_T	Rapidity	Isolation Cuts
Photon	$p_{T,\gamma}^{min} = 45$ GeV	$\lvert y_\gamma \rvert < 1.37$	$R = 0.4$, $E_T = 7$ GeV
	$p_{T,\gamma}^{max} = 1000$ GeV	$1.52 < \lvert y_\gamma \rvert < 2.37$	
Heavy Jet	$p_{T,Q}^{min} = 20$ GeV	$\lvert y_Q \rvert < 2.4$	$R_{jet} > 0.4, R_{Q\gamma} > 1$

Table 1: Cuts applied to the predictions shown in Figs. 5, 6.

$1.52 <\mid y_\gamma \mid < 2.37$. In this case larger - x values are probed and therefore we start to observe the difference between the solid and dashed (dash-dotted) lines at smaller p_T^γ values than in Fig. 5. The difference when using the BHPS IC PDFs is about 200% at $p_T^\gamma \sim 200$ GeV and increases almost up to 300% for $p_T^\gamma \sim 400$ GeV. In this rapidity region the difference between the BHPS and sea-like spectra is clearly visible even as early as $p_T^\gamma \sim 200$ GeV. However, while the IC is more accentuated, the cross-section and hence the number of events is less than those for the photon central rapidity in Fig. 5. For completeness in Fig. **??** we present the $\gamma + b$ cross-section .

3. Conclusion

It was shown that through direct photon production in association with a heavy quark we can study and constrain the heavy quark PDFs. More specifically measurements at the Tevatron of this process have indicated a possible existence of IC that seems to favor the BHPS model. Further tests at the LHC of this process especially at forward rapidities should be able to constrain or disfavor the presence of intrinsic charm in the proton.

References

[1] T. Stavreva, J.F. Owens, Phys. Rev. **D79**, 054017 (2009), [0901.3791 [hep-ph]].

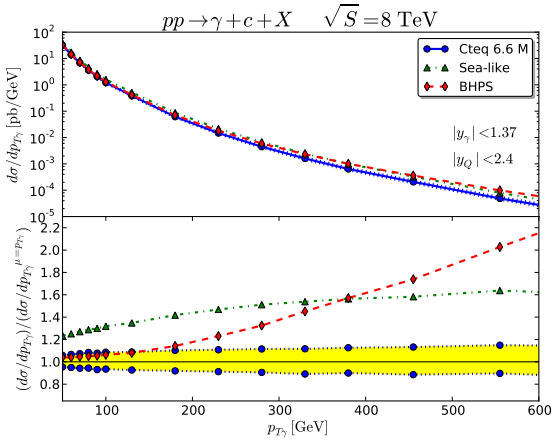

Figure 5: The $d\sigma/dp_T^\gamma$ distribution versus the transverse momentum of the photon for the process $pp \to \gamma + c + X$ at $\sqrt{s} = 8$ TeV using CTEQ6.6M (solid blue line), BHPS CTEQ6c2 (dashed red line) and sea-like CTEQ6c4 (dash-dotted green line), for central photon rapidity $|\, y_\gamma \,| < 1.37$ (top). The ratio of these spectra with respect to the CTEQ6.6M (solid blue line) distributions (bottom).

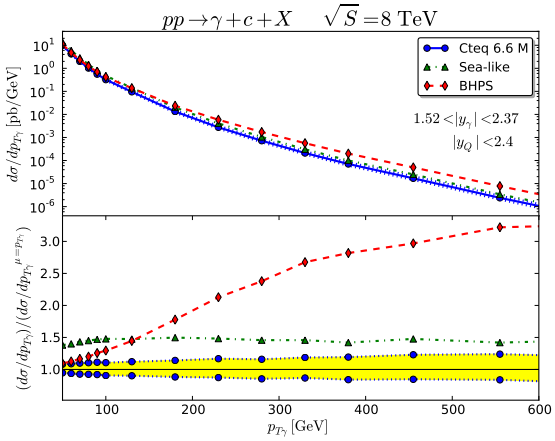

Figure 6: Same as Fig. 5 but at forward photon rapidity.

[2] J. J Aubert et al., [European Muon Collaboration], Nucl. Phys. **B213**, 31 (1983).

[3] S. J. Brodsky et al., Phys. Lett. **B93**, 451 (1980).

[4] F. S. Navarra et al., Phys. Rev. **D54**, 842 (1996).

[5] J. Pumplin et al., Phys. Rev. **D75**, 054029 (2007) [hep-ph/0701220].

[6] V. M. Abazov et al., [DØ Collaboration], Phys. Rev. Lett. **102**, 192002 (2009) [0901.0739 [hep-ex]].

[7] Aaltonen, T. *et al.,* Phys.Rev. D **81** (2010) 052006; arXiv:0912.3453 [hep-ex].

[8] V.M. Abazov, *et al.,* Phys.Lett. B **714** (2012) 32; arXiv:1203.5865 [hep-ex].

[9] V.A. Bednyakov et al., [1305.3548 [hep-ph]].

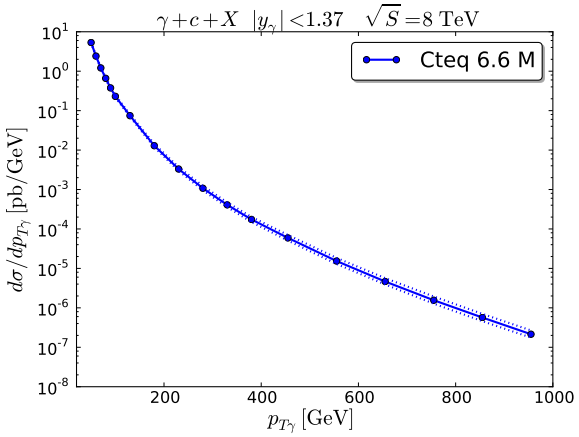

Figure 7: $\gamma+b$ differential cross-section.